Extremely confined quantum-well states for (2 × 2)-K and ($\sqrt{3}$ × $\sqrt{3}$)-K on graphite: First-principles calculations

V. Chis[1,2] and L. Walldén[2]

[1]*Donostia International Physics Center, E-20018 Donostia–San Sebastiàn, Spain*

[2]*Department of Applied Physics, Chalmers University of Technology, S-412 96 Göteborg, Sweden*

(Received 3 August 2011; revised manuscript received 26 September 2011; published 25 October 2011)

We report on the atomic and electronic structure obtained by *first-principles* density functional theory calculations for a (2 × 2)-K monolayer as well as a ($\sqrt{3}$ × $\sqrt{3}$)-K monolayer on graphite represented by an 11-layer carbon slab. In both cases, the calculations predict that the K atoms reside above hollows [2.93 Å above the surface atomic layers for (2 × 2)-K]. The electronic structure is characterized by a partially occupied, free-electron-like overlayer quantum-well (QW)-state band ($E_F - 0.76$ eV at $\bar{\Gamma}$, $1.14m_e$) and one empty QW band ($E_F + 1.7$ eV, $1.0m_e$), for (2 × 2)-K. The partially filled QW band, which has an energy and dispersion close to that which has been experimentally observed, provides examples of extremely confined states with nearly all charge (93%) deposited in the overlayer. In the substrate, the layer-confined σ bands are rigidly downshifted, by 0.6 eV for the outermost carbon-atom layer and by 0.14 eV for the second layer. For the π electrons, downshifted bands are split off from the ladder of closely spaced band energies, which approximate the continuum of states in a thick graphite sample. The splitting off can be regarded as the formation of a QW state, since the electrons are found mainly in the outermost layer of carbon atoms. The split-off band is not obtained via a downshift of the band with the lowest energy among the closely spaced states, since the band-edge states of the bare substrate have only a small amplitude in the outermost layer of carbon atoms. The high degree of confinement for both the K overlayer states and the C underlayer π states should make the system of interest for studies of the excitations of two near-two-dimensional electron gases at short distance.

DOI: 10.1103/PhysRevB.84.165449 PACS number(s): 73.20.At, 73.20.Hb, 73.21.Fg

I. INTRODUCTION

On some substrates, alkali-metal overlayers may form near-ideal two-dimensional (2D) electron gases. The strong confinement can be obtained if the substrate has a band gap, which allows quantum-well-like states in the overlayer to penetrate the substrate only with an oscillating tail. In such a case, and graphite is one, there may be a significant change also of the electronic structure in the substrate near its surface. For graphite, the change is from semimetal to metal character. The purpose of the present first-principles density functional theory (DFT) calculations is to characterize the electronic structure of this system. Also, as discussed below, the electron gas in the substrate is highly confined, such that one obtains a system with two separate electron gases in adjacent atomic layers uppermost in the sample.

Like in most previous works on alkali-metal-covered graphite, we study the K-graphite system, which forms a 2 × 2 ordered overlayer at full monolayer coverage. This structure has been determined via low-energy electron diffraction (LEED).[1] Thicker films can be grown, with relative ease, layer by atomic layer.[2–4] For the calculations, our substrate is an 11-atomic-layer-thick film of graphite. The adsorbate is a monolayer of K with either (2 × 2) or ($\sqrt{3}$ × $\sqrt{3}$) order. There are two reasons for including the latter structure. One is that the corresponding reciprocal lattice vector has actually been observed in an electron-scattering experiment,[5] and another is that we find that there is little energy difference between the two structures. One may note that the nearest distance between K atoms in K metal is intermediate between the distances in the two structures.

Previous photoemission studies have provided information about the electronic structure of the (2 × 2) ordered system and how this develops with increasing K monolayer coverage.[4,6] In recent works, the low monolayer coverage range has been focused for one or few layers of graphene, with one reason being that one expects the electronic structure of graphene or graphite in an electronics component to be modified much the same as by an external electric field.[7–11] Much attention has therefore been paid to the details of the intricate electronic structure near the Fermi level. The substrate is then often obtained as an overlayer. By heating SiC, one may prepare thin films of graphite[12] with a quality that gives well-resolved valence electron photoelectron spectra.[13]

II. CALCULATIONS

The atomic and electronic structure calculations were performed using the plane-wave package QUANTUM ESPRESSO,[14] based on the DFT. We adopt ultrasoft pseudopotentials[15] for K and C and the Perdew-Zunger[16] local-density approximation for the exchange and correlation energy.

The graphite substrate was modeled by a slab composed of 11 ($ABAB\ldots$) stacked graphene layers in a periodically repeated supercell. An optimized nearest-neighbor C-C distance of 1.420 Å was used for the graphene layers, and the interplanar distance was fixed at the experimental value of 3.354 Å.[17] The distance in vacuum separating the repeated graphite cells was set to 12 Å. The electronic structure was calculated by expanding the plane-wave basis to a cutoff of 30 Ry, and the effective potential and the charge density up to 160 Ry. The surface Brillouin-zone (SBZ) integration was performed with the Monkhorst-Pack scheme, adopting $\vec{k}$-point

meshes equivalent to a $(14 \times 14 \times 1)$ mesh in the irreducible SBZ of graphite, and a finite temperature smearing of the Marzari-Vanderbilt[18] type set to 0.03 Ry. The energy-band structure was calculated along the high-symmetry $\bar{K} - \bar{\Gamma} - \bar{M}$ direction of the SBZ, and sampling was performed over 130 $k_{\parallel}$ points.

The alkali-metal atoms were placed in the hollow positions on both sides of the slab. The supercells of $(\sqrt{3} \times \sqrt{3})$-K and (2×2)-K consist of 6 and 8 C atoms, respectively, in each layer. In order to marginalize surface-to-surface interaction through the vacuum region, the surfaces were separated by 25 Å of vacuum. The atomic arrangement of the $(\sqrt{3} \times \sqrt{3})$-K and (2×2)-K on the graphite surface was obtained by minimizing the total energy with respect to the positions of the K and the two topmost carbon layers. During the relaxation process, a (12×12) Monkhorst-Pack mesh was used and the criterion on the resulting forces was set to be less than 25 meV/Å.

III. RESULTS AND DISCUSSION

Even though the alkali adsorption is accompanied by a substantial rearrangement of charge, the substrate structure is only modestly affected. For the $(\sqrt{3} \times \sqrt{3})$-K as well as the (2×2)-K structure, the resulting relaxation of the first graphite layer with respect to the second layer is a contraction by 0.14%, according to our calculation. The distance between the second and third carbon layer is unaltered by the adsorption. The displacements in the lateral directions of the C atoms in the presence of K adsorption are on average only by 10^{-4} Å. Compared with previously reported LEED[17] experimental results, there is a good agreement regarding the K-graphite layer spacing for the (2×2)-K. The experimental value for the (2×2)-K system is 2.79 ± 0.03 Å, while our theoretical value is 2.9 Å, and for the $(\sqrt{3} \times \sqrt{3})$-K system, the distance is slightly larger, at 2.95 Å, than that of the (2×2)-K system. In addition, we have also calculated the binding energy per K atom in the two structures. The binding energy is defined as the amount of energy per K atom required to remove the atom from its equilibrium position on the graphite surface, with the final state being that of the clean graphite surface and the K atom isolated in vacuum. The binding energies for the two structures are very similar, namely, 1.14 eV per K atom for the (2×2)-K compared to 1.13 eV of the $(\sqrt{3} \times \sqrt{3})$-K structure. 1.14 eV agrees well with previously reported calculated values by Persson and Lamoen[19] of ~1 eV, while Manninen *et al.*[20] reports a value which is about a factor of 2 smaller (0.56 eV). One of the reason that our calculated binding energy per K atom differs compared to the one given by Manninen *et al.* might originate from the difference in the adsorption distance to the substrate of 3.17 Å compared to our calculated value of 2.9 Å.

The calculated electron energy-band structure of the 11-layer graphite substrate is presented in Fig. 1. The main signature of the surface band structure is the existence of a surface-state band located at $E_f + 3.8$ eV at the $\bar{\Gamma}$ point, indicated by the red solid lines in Fig. 1. There are two parabolic bands, due to the fact that there are two surfaces in our slab calculations, and the splitting between the two bands indicates the strength of the interaction between the surfaces.

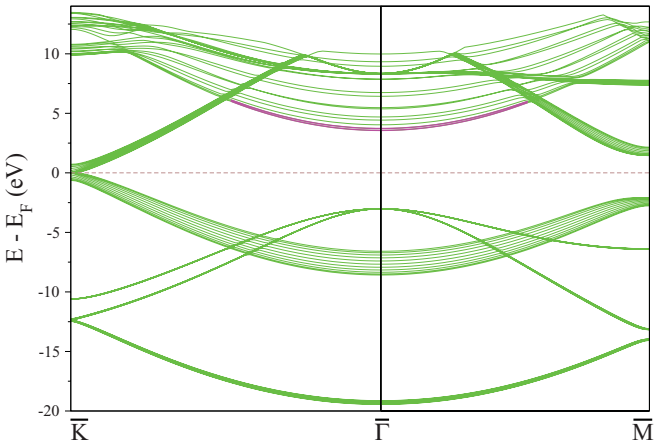

FIG. 1. (Color online) Calculated band structure for 11-atomic-layer graphite (0001) slab along the high-symmetry directions in the surface Brillouin zone. Binding energies are given with respect to the Fermi energy. Bands with thicker solid lines correspond to the graphite surface state (red line).

The surface state has a dispersion close to that of a free electron with an effective mass of $1.05m_e$. The planar-averaged squared wave function at $\bar{\Gamma}$ is shown in Fig. 2. The surface state [Fig. 2(a)] has almost its entire charge on the vacuum side of the first carbon layer and a fast decaying tail into the bulk region of the slab. This state has been noted in previous works[21,22] and is mentioned here to point out the similarity with the K overlayer quantum-well states discussed below. The wave function in Fig. 2(b) corresponds to the next higher $\bar{\Gamma}$ state in Fig. 1. This state has the characteristics of a bulk electronic state and deposits charge mainly in the deeper carbon layers. The energy is just below the vacuum level at 4.65 eV.

The charge-density redistribution for the $(\sqrt{3} \times \sqrt{3})$-K and (2×2)-K overlayer structures shown in Fig. 3 was obtained by summation of the charge-density distribution of a free-standing K monolayer and the graphite slab and subtraction of the sum from the charge-density distribution for the overlayer system. Shown in the left-hand panel of Fig. 3 is the plane-averaged charge redistribution along the

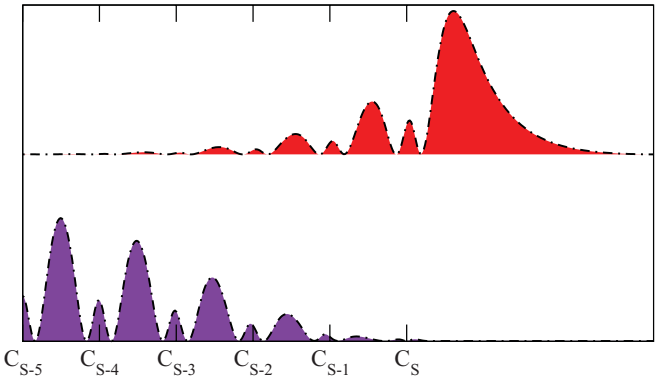

FIG. 2. (Color online) Plane-averaged squared wave functions along the surface normal corresponding to the graphite surface state, marked by thicker solid lines in Fig. 1, and the band above the surface state for comparison. The graphite atomic planes are indicated, where C_S marks the topmost graphite layer.

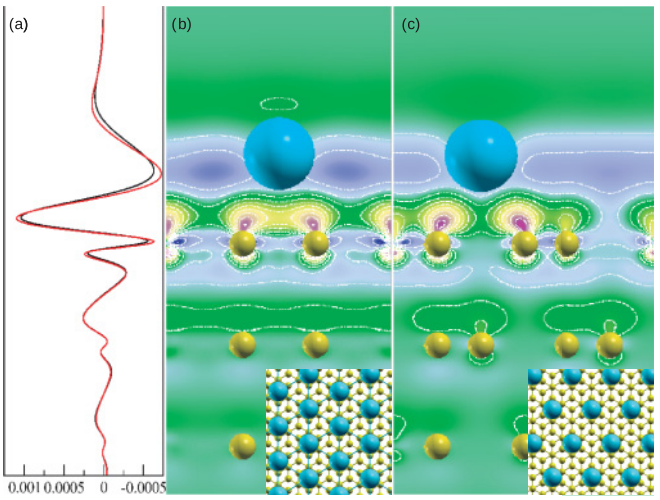

FIG. 3. (Color online) Calculated electron-density redistribution for $(\sqrt{3} \times \sqrt{3})$-K and (2×2)-K monolayer onto graphite (0001). (a) The redistribution for the plane-averaged quantity along the surface normal for both systems studied. (b) and (c) The redistribution of the electron density is shown in the $(11\bar{2}0)$ plane for $(\sqrt{3} \times \sqrt{3})$-K and (2×2)-K, respectively. In the lower parts, the top view of the respective structures is shown. The charge-density redistribution is given as change in electrons/a.u.

surface normal for both overlayer systems. In the right-hand panels, the redistribution of the charge is presented in the $(11\bar{2}0)$ cut plane for $(\sqrt{3} \times \sqrt{3})$-K and (2×2)-K, respectively. One notes that most of the charge accumulation is found in the interface region between the outermost carbon layer and the adlayer. The increase at the interface between the K and C layers is due mainly to charge transfer from the K layer. Moreover, Fig. 3 shows that there is also a significant charge transfer from the first graphite layer, which becomes depleted on the side toward the interior of the substrate. In addition, from Fig. 3 one notes that the adsorption affects the charge distribution in deeper carbon layers as well. The redistribution is similar in all layers, with charge accumulating on the side toward vacuum and depleting on the side toward the interior. There is more charge on the accumulation side and thus a net transfer of electrons to the deeper layers occurs. The maxima in Fig. 3 (left panel) decrease by a factor of around 3 between each layer, resulting in a screening depth somewhat less than the interplanar distance. The charge redistribution gives an induced dipole moment and a corresponding reduction in the work function, $\Delta\Phi$. The calculated work function of the graphite slab is 4.65 eV (experimental: 4.7 eV),[23] which is reduced by 2.05 and 2.22 eV when the K layer is adsorbed in a $(\sqrt{3} \times \sqrt{3})$-K and (2×2)-K overlayer structure, respectively. The experimental[4,23] value for (2×2)-K is somewhat lower (2.3 eV) than the one predicted (2.4 eV).

The calculated energy-band structures of the two overlayer systems are presented in Fig. 4. Indicated are two parabolic bands (denoted as $n = 1$ and $n = 2$ in the diagrams), which are formed by the two lowest QW states of the overlayer systems having one and two nodes in the overlayer, respectively. For the (2×2)-K structure (Fig. 4, right panel), the partially occupied, $n = 1$, QW-state band has its minimum $E_f - 0.76$ eV at $\bar{\Gamma}$ and disperses with an effective mass of $1.14m_e$. The QW-state band appears in a bulk projected energy gap at the SBZ $\bar{\Gamma}$ point, while the unoccupied, $n = 2$, QW state is located within a continuum of folded bulk bands. For the $(\sqrt{3} \times \sqrt{3})$-K system (Fig. 4, left panel) the $n = 1$ QW state is at $E_f - 1.08$ eV at the $\bar{\Gamma}$ point, while the $n = 2$ QW state is at $E_f + 1.53$ eV. The effective masses of the $n = 1$ and $n = 2$ QW bands are 1.22 and $0.8m_e$, respectively. The experimental values for the (2×2)-K structure obtained by angle-resolved photoemission are 0.57 eV for the filled band width and $1.1m_e$ for the dispersion.[6] In contrast to the (2×2)-K band structure, the $n = 2$ QW state now appears in a projected energy gap and the $n = 1$ QW state is within the folded bulk band continuum. The squared planar-averaged wave functions corresponding to the $n = 1$ and $n = 2$ QW states for the (2×2)-K are shown in Fig. 5 [the corresponding wave functions for the $(\sqrt{3} \times \sqrt{3})$-K have the same character and are not shown]. The states are extremely confined to the overlayer. Their tail decays rapidly into the graphite and, beyond the first graphite layer, the deposited charge is insignificant. For the $n = 1$ QW state of the (2×2)-K structure, 93% of the QW charge is

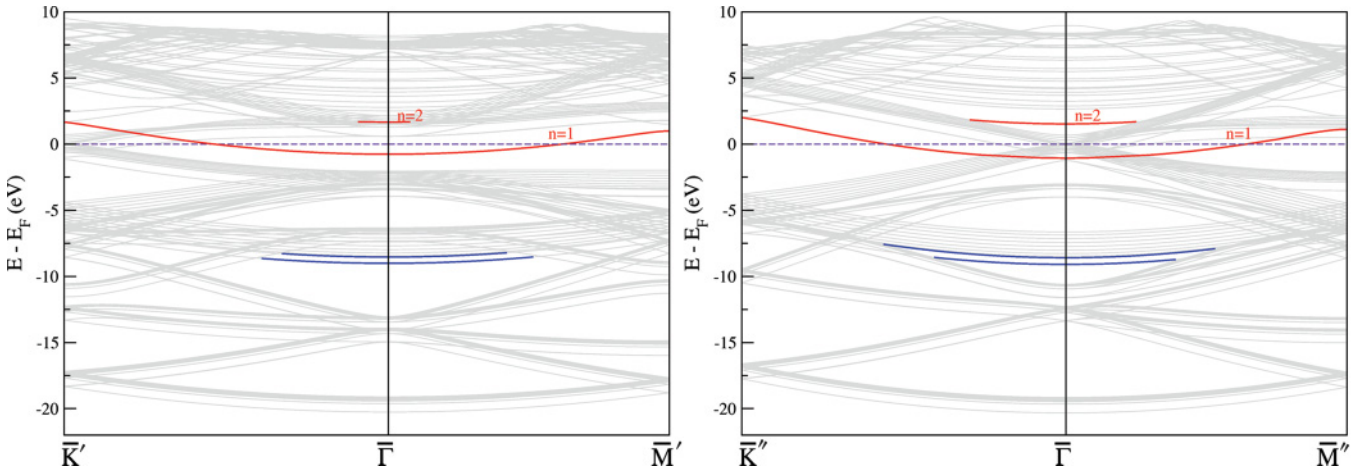

FIG. 4. (Color online) Band structure for the (2×2)-K and $(\sqrt{3} \times \sqrt{3})$-K monolayer on graphite surface along the SBZ high-symmetry lines. The blue lines illustrate the almost constant shift of the energy bands. The two red energy bands indicates the $n = 1$ and $n = 2$ QW-state bands, respectively.

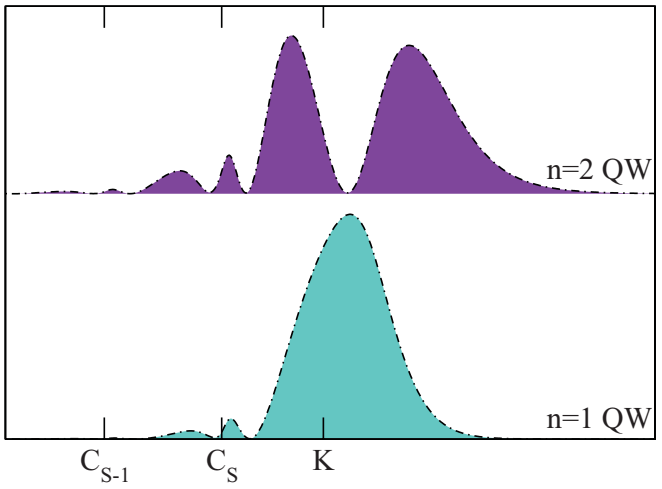

FIG. 5. (Color online) Plane-averaged squared wave functions along the surface normal for the $n = 1$ and $n = 2$ QW-state wave functions of the (2×2)-K systems. The potassium overlayer and the first two graphite planes are indicated.

deposited in the overlayer if this space is demarked by a plane half an interplanar distance outside the cores of the atoms in the outermost carbon layer. In addition to the characteristic QW-state bands of the overlayer system, we further notice bands belonging to the graphite substrate which are peeled off from their neighboring bands. Some of these bands have been indicated by blue (dark) lines in Fig. 4.

The $\bar{\Gamma}$ states of the two π bands highlighted in Fig. 4 (blue lines) deposit charge as shown in Fig. 6, where the squared wave function along the surface normal is presented. The wave function denoted as (a) in Fig. 6 corresponds to the lower blue band in Fig. 4. The state has most of its charge localized at the interface region and at the topmost carbon layers, consistent with the charge redistribution in Fig. 3. For comparison, the same quantity is plotted for the upper blue band of Fig. 4, denoted as (b) in Fig. 6. This state has bulk character but also acquires some weight in the interface region. In order to further illustrate the shift in the electron bands, we analyzed the projected density of states (PDOS) corresponding to different carbon layers. Shown in Fig. 7(a) is the total DOS of the (2×2)-K overlayer system, while Fig. 7(b) represents the projection of s states on the alkali overlayer (grey), first carbon layer (red), and second carbon layer (green), and Fig. 7(c) corresponds to the projection of p states on the first and second carbon layers, respectively. The rigid shift of the states belonging to the first carbon layer is clearly seen when the PDOS of the s and p states [Figs. 7(b) and 7(c)] is compared with the one belonging to the second carbon layer. In the grey curve corresponding to the s states of the overlayer, one notes several peaks with decreasing height toward higher energies. The two main peaks relate to the QW states of the (2×2)-K overlayer system in such a way that the QW states' energies at the $\bar{\Gamma}$ point fall at the low-energy side of the main peaks in the PDOS. In the inset of Fig. 7(b), we notice that at the same peak position as the main peak of the overlayer (grey curve) s states, an s-state peak belonging to the substrate also appears. This may be viewed

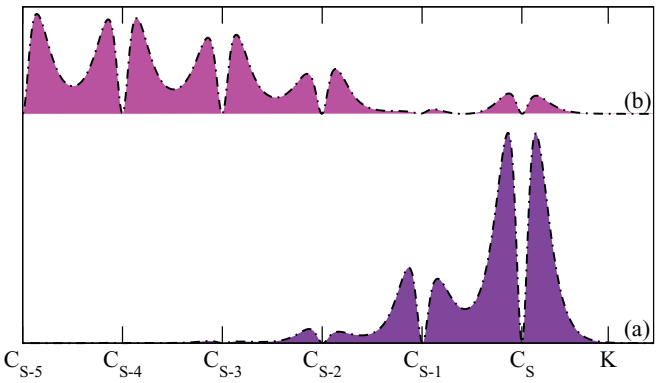

FIG. 6. (Color online) Plane-averaged squared wave functions along the surface normal. The graphite atomic planes and the alkali-atom positions are indicated. $\bar{\Gamma}$ π states of the bands marked blue in Fig. 4: (a) the lower band and (b) the upper band.

as a residue of the surface state of the clean graphite after it has hybridized with the lowest state of potassium to form the $n = 1$ QW state. This picture is further validated by comparing the plane-averaged squared wave function of the clean surface state (Fig. 2) and the QW state (Fig. 5). The similarities of the two are their extension in space and their oscillating tail into the substrate.

Recent angle-resolved photoemission spectroscopy (ARPES)[24] studies of coverages in the range of 0.26 monolayer to multilayers of K onto graphite have focused on the band structure around the Brillouin-zone corner ($\bar{K}$ point). The experimental results show that the π band near E_F at the $\bar{K}$ point shifts to higher binding energies upon K deposition. It

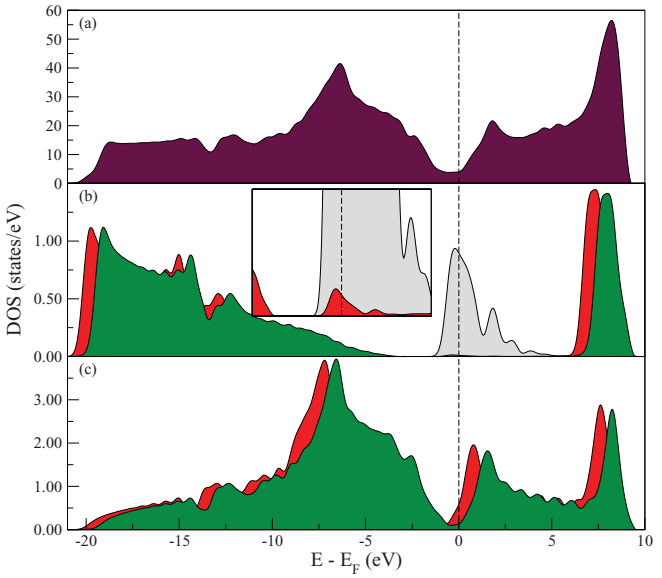

FIG. 7. (Color online) (a) Total density of states for the (2×2)-K overlayer system. Projected density of states: (b) s states projected on the K layer (grey), the first carbon layer (red), and the second carbon layer (green), respectively; (c) p states for first (red) and second (green) carbon layers, respectively. The inset in (b) corresponds to a focused region from -5 to 5 eV around the E_f and in the PDOS.

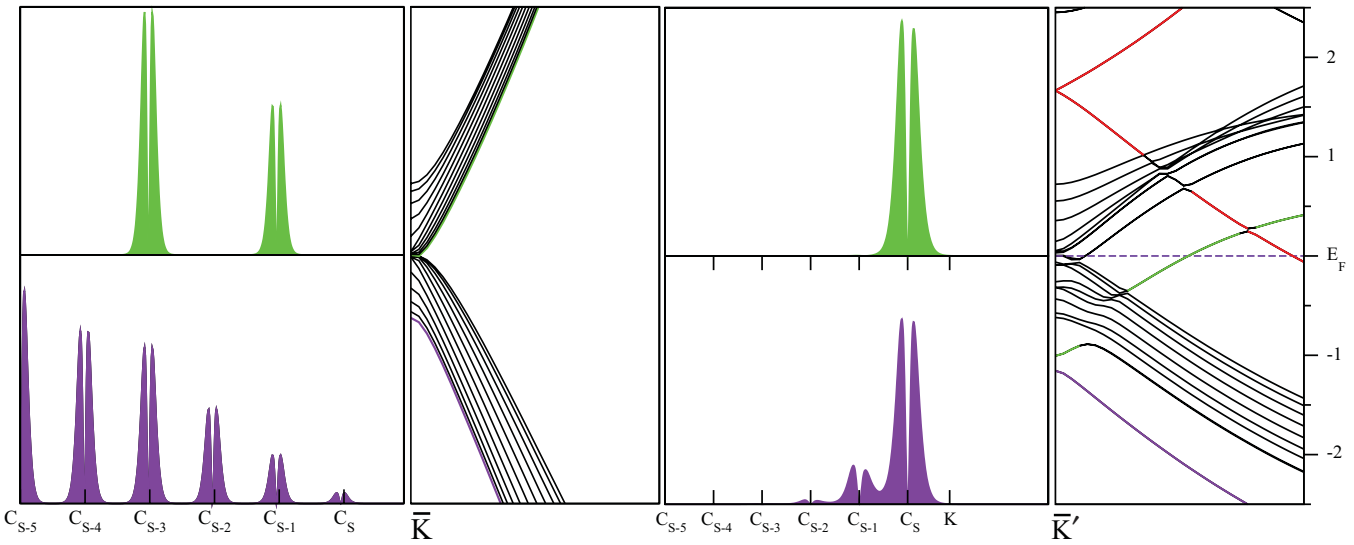

FIG. 8. (Color online) Band structure of the clean graphite surface and the (2×2)-K structure in the vicinity of the SBZ $\bar{K}$ point. Planar-averaged wave-function charge-density distribution along the surface normal corresponding to the indicated bands in the band structures.

is reported that for a K coverage of 0.26 monolayer on highly oriented pyrolytic graphite (HOPG), the π band, which for the clean surface lies very close to E_F, shifts to binding energies of $\sim$0.45 eV. In addition, the authors report an opening of a gap between the π and π^* bands at the $\bar{K}$ point. We are able to give further insight into these results. For a more detailed analysis of the gap opening and the shifted bands at the $\bar{K}$ point, we present in Fig. 8 the band structure of the clean and the (2×2)-K overlayer surface at the BZ $\bar{K}$ point, respectively. In the left panel of Fig. 8, the band structure of the clean graphite surface together with the planar-averaged squared wave function along the surface normal of the lowest π band and the lowest π^* band is shown. The choice of the two lowest bands belonging to the manifold of the π bands and π^* bands, respectively, is arbitrary. The squared wave function corresponding to the lowest π band distributes charge on all of the carbon layers with an amplification on the layers toward the slab center, while the distribution corresponding to the π^* band is more selective regarding the choice of layers. With the aid of our calculations, the experimental results[24] may be interpreted in terms of a lower gap boundary formed by the two bands shown in Fig. 8, where the squared wave function of the two bands is presented. In the right-hand panel of Fig. 8, we show the band structure of the (2×2)-K overlayer on graphite at the $\bar{K}$ point. The squared wave function at this point of the two bands that forms the lower boundary of the gap is shown in Fig. 8. As mentioned previously, owing to the adsorption of the K overlayer, there is a rigid shift in the bands corresponding to the first and second graphite layers. That is, the gap at the $\bar{K}$ point is formed between the downshifted π and π^* band and the remainder of the nearly degenerate bands around E_F. The size of the gap formed by the described bands is about 0.4 eV wide and the shifted bands are located at -1.01 eV (π^*) and -1.16 eV (π), respectively, for the (2×2)-K structure. By comparing the charge-density distribution at the π and π^* bands to that of the clean graphite surface, we note a redistribution of the charge with most of the amplitude on the first graphite layer.

The bands around the Fermi level for the clean surface at the $\bar{K}$ point occupy a width of 1.35 eV around E_F. By comparing to the band width of the (2×2)-K overlayer, we can conclude that the bands around E_F occupy the same width, namely, 1.34 eV. This confirms that a certain net transfer of free carriers from the K overlayer to the graphite substrate has taken place, and these are now accommodated by the downshifted bands and the characteristic QW state.

IV. CONCLUSIONS

We have presented a thorough analysis of the electronic structure of the (2×2) and the $(\sqrt{3} \times \sqrt{3})$ potassium overlayers onto graphite, calculated within the density functional theory framework. Both structures are characterized by a quasi-two-dimensional free-electron-like electron gas formed by the overlayer QW states. This resides on top of a second 2D free-electron-like electron gas due to the downshifted electronic states in the topmost graphite layer. In addition, we give a detailed description of the gap opening at the SBZ corner observed in experimental studies.[24] The gap at the SBZ corner is created by the downshifted π and π^* electronic bands, which are now decoupled from the manifold of bands surrounding the Fermi level. The downshifted π^* band, which now crosses the Fermi level toward the SBZ center, signals a net transfer of free carriers between the alkali overlayer and the topmost substrate layer.

Finally, we suggest that the high degree of confinement for both the K overlayer states and the C underlayer π states should make the system of interest for studies of the excitations of near-2D electron gases at short distances.

[1]R. D. Diehl and R. McGrath, Surf. Sci. Rep. **23**, 43 (1996).
[2]M. Caragiu and S. Finberg, J. Phys. Condens. Matter **17**, R995 (2004).
[3]N. Ferralis, K. Pussi, S. E. Finberg, J. Smerdon, M. Lindroos, R. McGrath, and R. D. Diehl, Phys. Rev. B **70**, 245407 (2004).
[4]M. Breitholtz, T. Kihlgren, S.-Å. Lindgren, and L. Walldén, Phys. Rev. B **66**, 153401 (2002).
[5]K. M. Koch and R. E. Palmer, Surf. Sci. **284**, 349 (1993).
[6]J. Algdal, M. Breitholtz, T. Kihlgren, S.-Å. Lindgren, and L. Walldén, Phys. Rev. B **73**, 165409 (2006).
[7]S. Y. Zhou, G.-H. Gweon, C. D. Spataru, J. Graf, D.-H. Lee, S. G. Louie, and A. Lanzara, Phys. Rev. B **71**, 161403R (2005).
[8]S. Y. Zhou, G.-H. Gweon, and A. Lanzara, Ann. Phys. **321**, 1730 (2006).
[9]S. Y. Zhou, G.-H. Gweon, J. Graf, A. V. Federov, C. D. Spataru, R. D. Diehl, Y. Kopelevich, D.-H. Lee, S. G. Louie, and A. Lanzara, Nature Phys. **2**, 595 (2006).
[10]A. Bostwick, T. Ohta, J. L. McChesney, K. V. Emtsev, T. Seyller, K. Horn, and E. Rotenberg, New J. Phys. **9**, 385 (2007).
[11]T. Ohta, A. Bostwick, T. Seyller, K. Horn, and E. Rotenberg, Science **313**, 951 (2006).
[12]I. Forbeaux, J.-M. Themlin, and J.-M. Debever, Phys. Rev. B **58**, 16396 (1998).
[13]T. Kihlgren, T. Balasubramanian, L. Walldén, and R. Yakimova, Phys. Rev. B **66**, 235422 (2002).
[14]P. Giannozzi, S. Baroni, N. Bonini, M. Calandra, R. Car, C. Cavazzoni, D. Ceresoli, G. L. Chiarotti, M. Cococcioni, I. Dabo, A. Dal Corso, S. de Gironcoli, S. Fabris, G. Fratesi, R. Gebauer, U. Gerstmann, C. Gougoussis, A. Kokalj, M. Lazzeri, L. Martin-Samos, N. Marzari, F. Mauri, R. Mazzarello, S. Paolini, A. Pasquarello, L. Paulatto, C. Sbraccia, S. Scandolo, G. Sclauzero, A. P. Seitsonen, A. Smogunov, P. Umari, and R. M. Wentzcovitch, J. Phys. Condens. Matter **21**, 395502 (2009).
[15]We have used the pseudopotentials C.pz-rrkjus.UPF and K.pz-n-vbc.UPF from [http://www.quantum-espresso.org].
[16]J. P. Perdew and A. Zunger, Phys. Rev. B **23**, 5048 (1981).
[17]K. R. Kganyago and P. E. Ngoepe, Phys. Rev. B **68**, 205111 (2003).
[18]N. Marzari, D. Vanderbilt, A. DeVita, and M. C. Payne, Phys. Rev. Lett. **82**, 3296 (1999).
[19]D. Lamoen and B. N. J. Persson, J. Chem. Phys. **108**, 3332 (1998).
[20]K. Rytkönen, J. Akola, and M. Manninen, Phys. Rev. B **75**, 075401 (2007).
[21]M. Posternak, A. Baldereschi, A. J. Freeman, and E. Wimmer, Phys. Rev. Lett. **52**, 863 (1984).
[22]T. Fauster, F. J. Himpsel, J. E. Fischer, and E. W. Plummer, Phys. Rev. Lett. **51**, 430 (1983).
[23]L. Österlund, D. V. Chakarov, and B. Kasemo, Surf. Sci. **420**, 174 (1999).
[24]N. Kamakura, M. Kubota, and K. Ono, Surf. Sci. **602**, 95 (2008).